

# Design and Manufacturing of High Performance, Reduced Charge Heat Exchangers



Mingkan Zhang  
Daniel Bacellar  
Jiazhen Ling  
Vikrant Aute  
James Tancabel  
Yoram Shabtay  
Jan Muehlbauer  
Jiazhen Ling  
Zhenglai Shen  
Patrick Geoghegan  
Omar Abdelaziz

**December 31, 2022**

## DOCUMENT AVAILABILITY

Reports produced after January 1, 1996, are generally available free via US Department of Energy (DOE) SciTech Connect.

**Website** <http://www.osti.gov/scitech/>

Reports produced before January 1, 1996, may be purchased by members of the public from the following source:

National Technical Information Service  
5285 Port Royal Road  
Springfield, VA 22161  
**Telephone** 703-605-6000 (1-800-553-6847)  
**TDD** 703-487-4639  
**Fax** 703-605-6900  
**E-mail** [info@ntis.gov](mailto:info@ntis.gov)  
**Website** <http://classic.ntis.gov/>

Reports are available to DOE employees, DOE contractors, Energy Technology Data Exchange representatives, and International Nuclear Information System representatives from the following source:

Office of Scientific and Technical Information  
PO Box 62  
Oak Ridge, TN 37831  
**Telephone** 865-576-8401  
**Fax** 865-576-5728  
**E-mail** [reports@osti.gov](mailto:reports@osti.gov)  
**Website** <http://www.osti.gov/contact.html>

This report was prepared as an account of work sponsored by an agency of the United States Government. Neither the United States Government nor any agency thereof, nor any of their employees, makes any warranty, express or implied, or assumes any legal liability or responsibility for the accuracy, completeness, or usefulness of any information, apparatus, product, or process disclosed, or represents that its use would not infringe privately owned rights. Reference herein to any specific commercial product, process, or service by trade name, trademark, manufacturer, or otherwise, does not necessarily constitute or imply its endorsement, recommendation, or favoring by the United States Government or any agency thereof. The views and opinions of authors expressed herein do not necessarily state or reflect those of the United States Government or any agency thereof.

Energy and Transportation Sciences Division

**Design and Manufacturing of High Performance, Reduced Charge Heat Exchangers**

Authors:

Mingkan Zhang  
Daniel Bacellar  
Vikrant Aute  
James Tancabel  
Yoram Shabtay  
Jan Muehlbauer  
Jiazhen Ling  
Zhenglai Shen  
Patrick Geoghegan  
Omar Abdelaziz

Date Published: November 30, 2022

Prepared by  
OAK RIDGE NATIONAL LABORATORY  
Oak Ridge, TN 37831-6283  
managed by  
UT-BATTELLE, LLC  
for the  
US DEPARTMENT OF ENERGY  
under contract DE-AC05-00OR22725



## CONTENTS

LIST OF FIGURES .....	iv
ABSTRACT.....	1
1. INTRODUCTION .....	1
2. FRAMEWORK OF FATIGUE ANALYSIS .....	2
3. FATIGUE ANALYSIS OF SINGLE TUBES.....	4
4. STRESS ANALYSIS OF HEADERS.....	7
5. EFFECTS OF UNPERFECT FITTING OF THE SPACER AND TUBE .....	9
6. FATIGUE ANALYSIS OF ASSEMBLED HEAT EXCHANGERS. ....	14
7. SUMMARY .....	19
REFERENCES.....	19

## LIST OF FIGURES

Figure 1. A typical design of non-round shaped heat exchanger. ....	2
Figure 2. The experimental (a) and numeral (b) setups of the deformation test. ....	3
Figure 3. The comparison of deformation results. ....	3
Figure 4. Life repeats VS stress scale for different designs with different materials. ....	4
Figure 5. Contours for log value of the life repeats using Copper. ....	5
Figure 6. Contours for log value of the life repeats using Aluminum. ....	6
Figure 7. Different cross-sections of the headers. ....	7
Figure 8. Stress distributions in 3 headers. ....	7
Figure 9. A schematic view of the header depth study. ....	8
Figure 10. Stress distributions at the same cross-section of 3 headers with different size. ....	9
Figure 11. A case with 1.5 degrees rotation of the tube from the original orientation. ....	10
Figure 12. Stress distribution in the solder with original orientation. ....	11
Figure 13. Stress distribution in the solder with 1.5 degrees rotation. ....	11
Figure 14. Plastic stress VS plastic strain for SAC 396 and copper. ....	12
Figure 15. Plastic stress on the solder using SAC 396. ....	12
Figure 16. Plastic strain on the solder using copper. ....	13
Figure 17. Schematic view of the heat exchange model. ....	14
Figure 18. Three shapes of the tubes and fillers. ....	15
Figure 19. Stress distributions on the tubes with three shapes. ....	16
Figure 20. Stress distributions on the fillers with three shapes. ....	16
Figure 21. Stress distributions on the headers with three shapes. ....	17
Figure 22. Fatigue analysis results showing life repeats vasus stress scale of the heat exchangers with three tube shapes. ....	18

## **ABSTRACT**

A framework of stress analysis and fatigue analysis was developed. Utilizing the framework, stress analysis and fatigue analysis of high-performance heat exchangers with non-round shaped tubes were studied. The tubes, headers and welding layers were studied separately before analyzing the assembled heat exchangers. Results reveal different stress strength on the different shapes of tubes and headers. Unevenly welding distribution is also discussed in the report. Moreover, the fatigue analysis results of the heat exchanger are helping to estimate the lifetime of the heat exchanger from fatigue point of view.

## **1. INTRODUCTION**

As one of the key components, air-to-refrigerant heat exchangers are widely implemented in vapor compression-based HVAC&R systems. As a result, the performance of such HVAC&R systems highly depends on the heat exchangers' performance. One of the approaches to enhance the performance of heat exchangers is to reduce the air-side heat transfer resistance [1]. Studies have been conducted to seek solutions to minimize the airflow resistance. On the other hand, from aerodynamics point of view, airfoils are the shapes providing much lower resistance than the round shape [2], which encourages studies to seek the shape-optimized tube to minimize the air-side resistance of heat exchangers [3–5]. Studies about tube shapes optimization for air-to-refrigerant heat exchangers have been reviewed by Tancabel et al. [6]. Consequently, it can be concluded that small diameter non-round shape- optimized tubes can significantly reduce the air-side resistance and improve the performance of such heat exchangers [5,7,8].

This project builds on earlier work that resulted in 20% reduced/improved designs and next logical step is to fully explore, full size prototyping and development for the most exciting discovery: tubes with shape-optimized cross sections (for example: droplet shape) leading to acceptable face area while meeting or exceeding all other component performance improvements by 25% (volume and weight). The project emphasizes on the design of air-to-refrigerant heat exchangers with 40% charge reduction while maintain the structural strength; manufacturing of tubes and joining them using novel minimal-charge headers; fabrication and testing of these new heat exchangers at component and system levels. The project will conduct design optimization of non-round tube heat exchangers with fins if sufficiently small tubes for finless design are not manufacturable. These heat exchangers are targeted towards residential and light commercial sector for new construction and retrofit applications. The heat exchanger design framework will be applicable to other heat exchangers in heating, ventilation, air conditioning and refrigeration (HVAC&R) industry independent of the refrigerant choice. The project will be divided into three phases with each phase lasting for one year. The first phase of the project aims to obtain optimal (in terms of both heat transfer performance and structural reliability) designs of small-diameter non-round tubes. Building upon the previous project, the optimization framework will include an FEM/FEA analysis along with the traditional air-side heat transfer and pressure drop analysis. Heat exchanger manufacturing challenges such as non-round tube extrusion and tube/header integration will also be comprehensively studied.

## 2. FRAMEWORK OF FATIGUE ANALYSIS

Previous studies have revealed that the HX with non-round shaped tubes showing can offer a low air-side heat transfer resistance and high heat transfer performance (Bacellar et al. 2016, 2017; Huang et al. 2016). The FEA modeling in present work was developed based on heat exchangers developed by University of Maryland. Figure 1 shows a typical design of the heat exchanger with non-round shaped tubes, which is comprised of tubes, headers, and spacer to support tubes and headers.

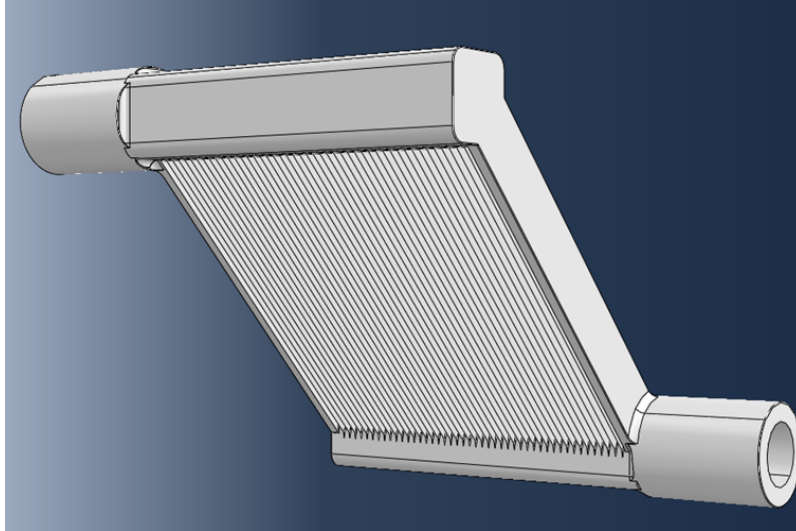


*Figure 1. A typical design of non-round shaped heat exchanger.*

A framework of fatigue analysis has been developed to analyze the stress distribution and fatigue risk of the non-round shaped heat exchangers. Here shows the steps of the framework:

- The designs were digitalized by using CAD software SOLIDWORKS, where the geometry files were created.
- Then the files were imported by Abaqus, in which the simulation domain were defined (single tube simulation or entire HX simulation), the constrains were assigned (Tie between header and solder, and between solder and tube), the boundary conditions and loads were set (6 MPa or 3.45 MPa baseline at the inner tube wall and header), and the mesh were created.
- After the model setup finished, the stress analysis simulations were running.
- Finally, the stress analysis results were read by fe-safe to run fatigue analysis.

The fatigue analysis relies on fatigue properties which are usually collected by experimental tests. To analyze the materials whose test data are not available, fatigue properties can be approximated using the Approximate Material Function. This function uses Bäuml-Seeger's method (Bäuml, Seeger, and Boller 1990) to generate approximate fatigue parameters based on the ultimate tensile strength (UTS) and elastic modulus of the material.

To validate the stress analysis modeling, a comparison between the numerical model results to the experimental data. The experimental setup is shown in Figure 2 (a). A single tube was tested by injecting pressurized gas from one of the ends of the tube, while the other end of the tube was sealed. The material of the tube was either copper or aluminum. The distance between the highest and lowest points of the tube was measured before and after pressurization, indicating the deformation of the tube. The highest pressure applied was up to 200 bar. A significant deformation was observed after the highest pressure was applied. To mimic the experimental setup, a numerical model about pressurized single tube was developed as shown in Figure 2 (b). After pressures applied to the tube, deformations in the model were measured and compared



to the experimental data. Figure 3 depicts the comparison results by using aluminum. The validation shows a very good agreement between numerical model results to the experimental data. After the stress analysis modeling has been successfully validated, the framework of fatigue analysis was implemented the heat exchangers.

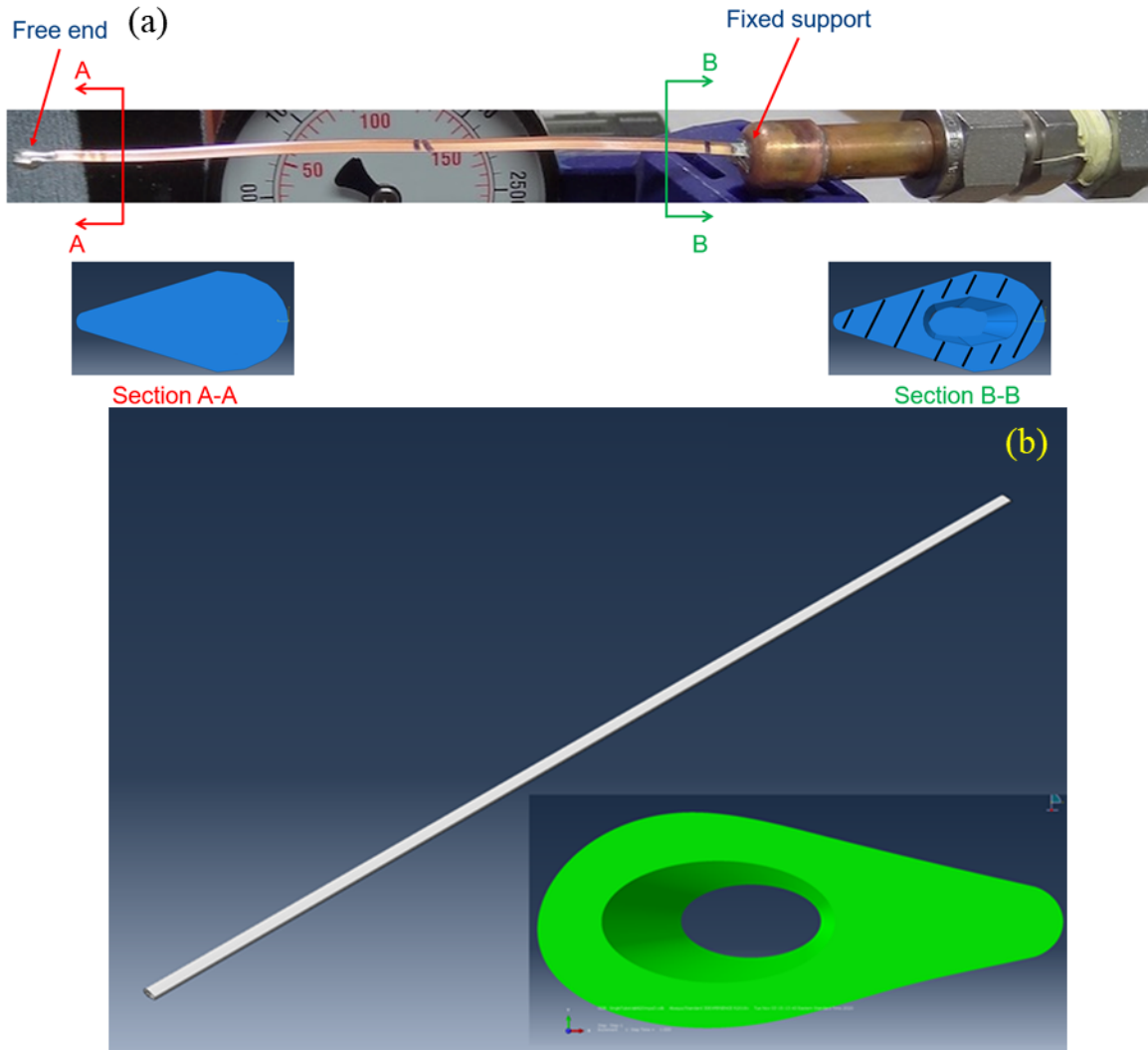


Figure 2. The experimental (a) and numeral (b) setups of the deformation test.

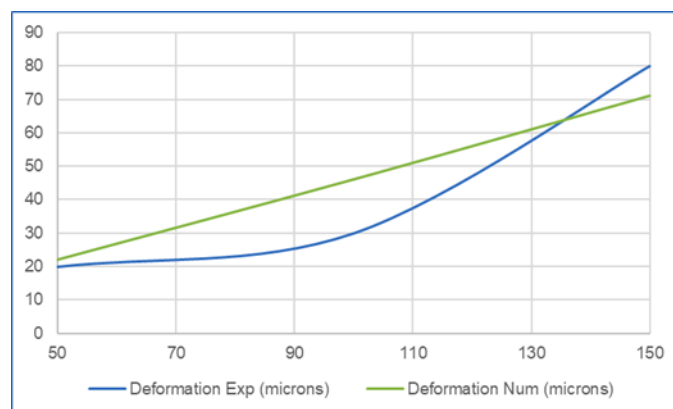


Figure 3. The comparison of deformation results.

### 3. ANALYSIS OF SINGLE TUBES

The framework was firstly utilized to conduct fatigue analysis of single tube. In this section, four kinds of tubes of two materials (Al6061-T6 forging and 99.99% Copper), which have different cross-section designs with either one hole or two separate holes of the tube, are studied. The baseline loading is 6 MPa pressure applied to the inner surfaces of the tubes to mimic the hydraulic pressure caused by the static and dynamic pressures from the refrigerants. Since saturation pressure varies with types of refrigerants, in the fatigue analysis, the loading was scaled up to 10 times. Note that the stress scale-up is the operation of fatigue analysis only, so in stress analysis only baseline loading needs to be simulated, which significantly reduces the total simulation time of the framework. The loading was periodically applied to the tube. For example, in one loading cycle, the applied pressure is from the scaled loading (12 MPa if scaled up to 2) to zero, then that back to the scaled loading starts the next loading cycle. After fatigue analysis accomplished, it returned a result called “life repeats”, which is the number loading cycles the tube experiences until the first failure occurs, indicating the lifetime of the part.

Figure 4 shows the life repeats change with loading scale, in which Aluminum and Copper indicates Al6061-T6 forging and Copper. Note that the maximum loading cycles in the fatigue analysis are  $10^8$ , so the data are not shown if the failure cycles are greater than  $10^8$ . Figure 4 indicates that all the tubes are able to bear more than  $10^8$  loading cycles without failure under the baseline loading. The dashed, and solid lines indicate the curves from tubes made of Al6061-T6 forging, and 99.99% Copper, respectively. It shows that curves from Copper, have slopes gentler than the Aluminum alloy. As a result, the lifetimes of 99.99% Copper tubes are less than Al6061-T6 forging when the loading scale is low. However, when the loading scale increases, 99.99% Copper tubes can last more cycles than Al6061-T6 forging does.

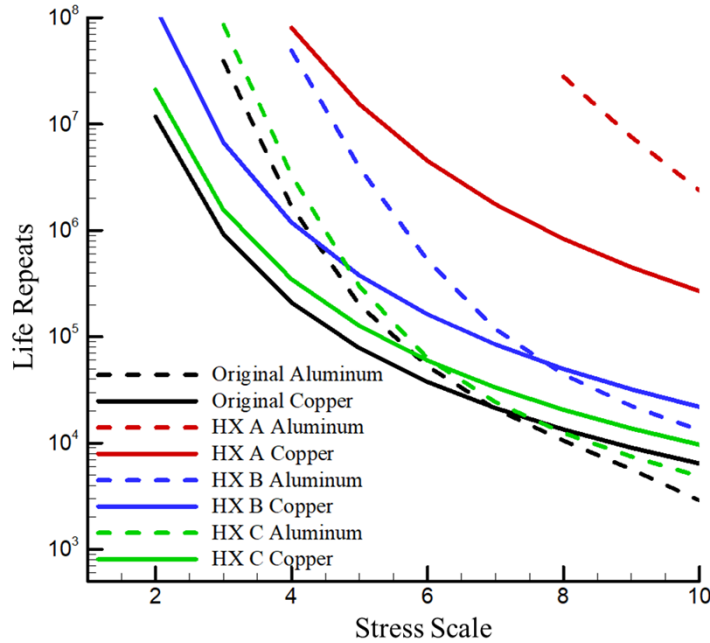


Figure 4. Life repeats VS stress scale for different designs with different materials.

In Figure 4, the black, red, blue, and green colors represent the results for original design, design A, design B, and design C tubes, respectively. Figures 5 and 6 depict contours for log value of the failure cycles when the loading scale = 10 for Al6061-T6 forging and 99.99% Copper, respectively. By comparing original design and design C, it can be found that design C improves the original design by expanding the hole and change the ellipse shape to a polygon. From Figure 4, only a little improvement from the original design to design C can be observed. Figure 5 shows that for original design, the lowest failure cycles happen

at the two ends of the ellipse shape hole. When design C improves the ellipse shape to a polygon, it absorbs some stress to the sides of the hole. However, the lowest lifetime still occurs at the two ends of the hole in design C. It explains why only little improvement from original design to design C has been observed.

From Figure 4, one can identify that the lifetimes of the tubes with double-hole cross-section (design A and B) are much greater than the ones with single-hole (original design and design C). It is because, in the double-hole designs, an extra structure is in the middle of the cross-section to support the tubes, leading to a stronger tube and longer lifetime. The contours of design C in Figure 5 and Figure 6 show the extra structure shares the load which significantly increases the lifetimes at the two ends of the ellipse shape hole comparing to the original design.

Figure 4 also indicates that design A is much better than B from the point of view of lifetime. Figure 5 and Figure 6 reveal that low lifetime happens at the corners of the cross-section geometry in design B, implying stress concentrations at the corners. On the other hand, because design A employs two round holes, the problem of stress concentration is conquered. As a result, design A has a much greater lifetime than design B. The locations where lowest lifetime of design A occurs can be identified by Figure 5, which is because the tube is thin at these locations.

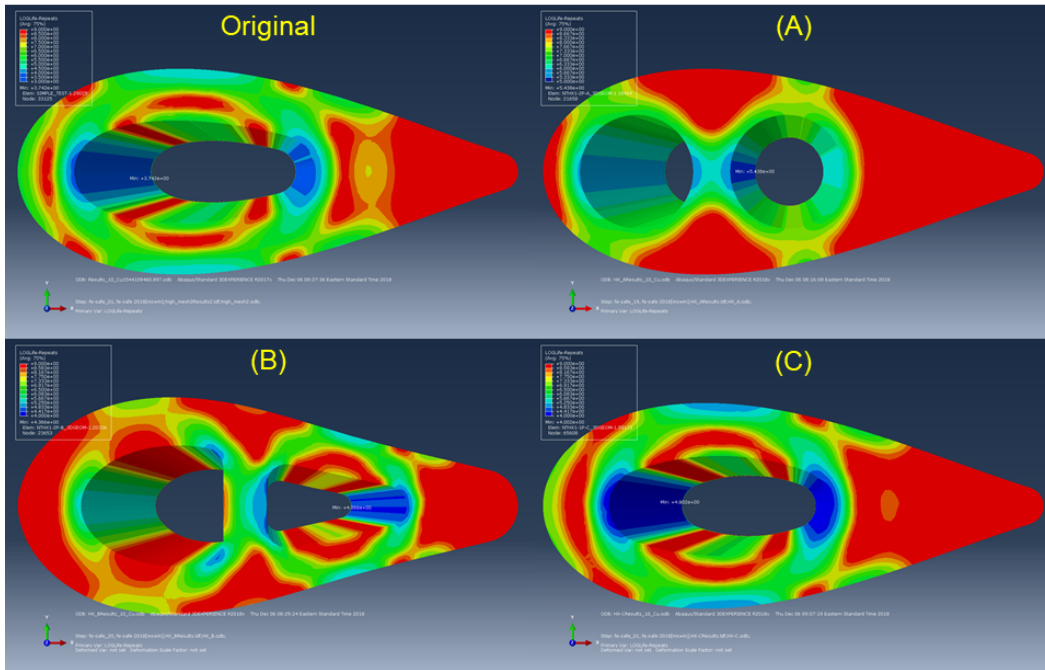


Figure 5. Contours for log value of the life repeats using Copper.

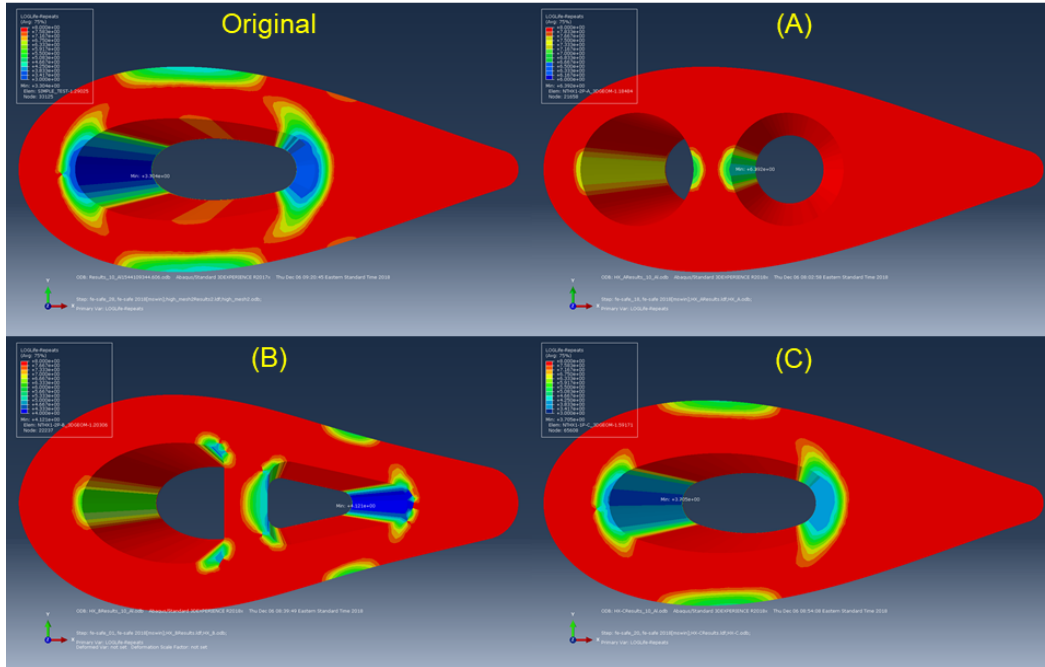


Figure 6. Contours for log value of the life repeats using Aluminum.

#### 4. STRESS ANALYSIS OF HEADERS.

After the stress and fatigue analysis on single tubes finished, stress analysis of headers was conducted, in which the effects of header's shape on the header stress have been studied. In addition to the shape effects, the depth of the reservoir in the header was also discussed.

##### ***EFFECTS OF THE HEADER'S SHAPE ON THE HEADER STRESS***

The stress analysis model was implemented to study the effects of the header's shape on the header stress. The cross-sections are square, half round, and round which are showing in Figure 7. The material is Copper. After 3.45 MPa is applied to all the headers, simulations were running to obtain the stress in the headers as shown in Figure 2. The results indicate that for all shapes, the stress concentration happens at the same place of the header's inner surface. However, after comparing the stress magnitude, one can find that the round shape has the lowest maximum stress, which is about 115 MPa, while the square one has the highest maximum stress, about 540 MPa. The half round shape also can significantly reduce the maximum stress on the header. The results indicate a round shape can be used to avoid high stress concentration in the header.

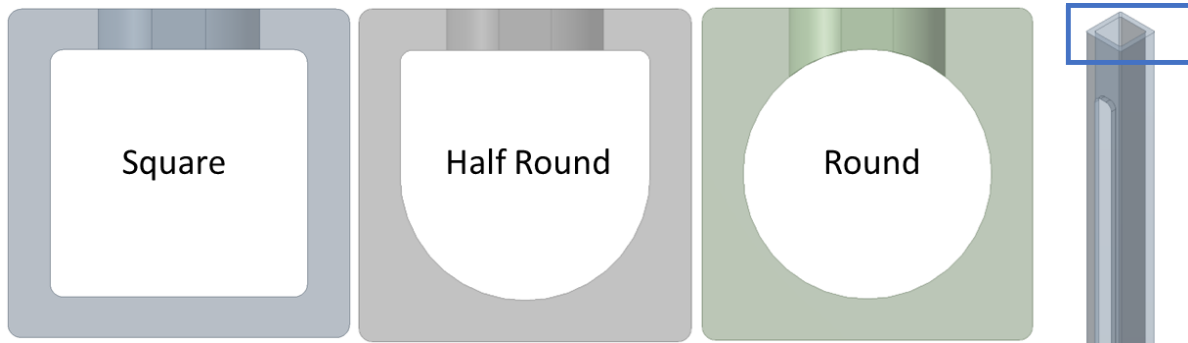


Figure 7. Different cross-sections of the headers.

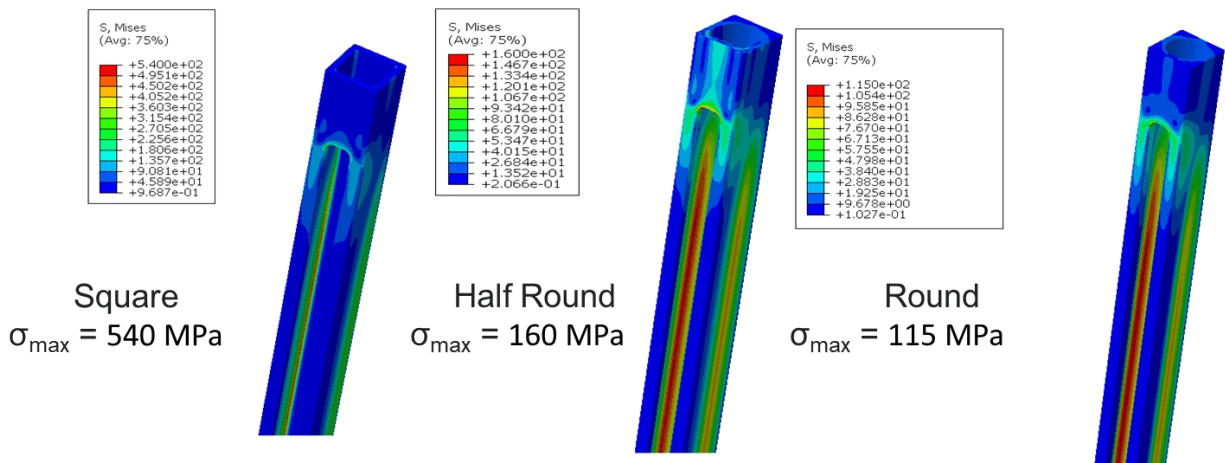
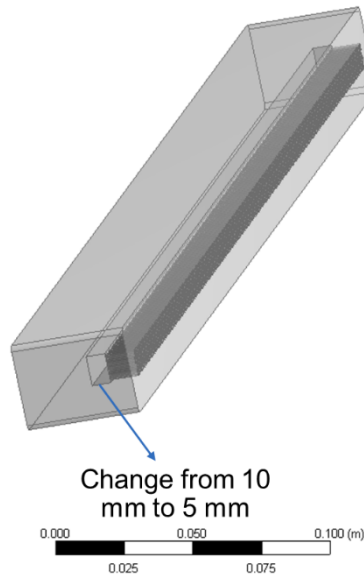


Figure 8. Stress distributions in 3 headers.

### ***EFFECTS OF THE HEADER'S VOLUME ON THE HEADER STRESS***

The stress analysis model was implemented to study the effects of the header's volume on the header stress. Since the length and height of the header cannot be changed due to the tubes, the only parameter that can be changed is the width of the header as shown in Figure 9. Therefore, 3 stress analysis cases were designed,  $w = 10$  mm, 7.5 mm and 5 mm, respectively to study the header size effects on the stress distribution. 500 psi (3.44 MPa) pressure is applied to all 3 headers. Figure 10 indicates the stress distributions at the same cross-section of 3 headers with different size. The maximum stress on the 10 mm, 7.5 mm and 5 mm headers are 16.8, 16.73 and 14.95 MPa, respectively. Since it does not make sense to test a smaller header, it can be concluded that no significant stress difference can be observed when the  $w$  changes from 10 mm to 5 mm. Therefore, on the header design, if a smaller header is desired, the designer can just focus on other trade-offs, e.g. pressure drop and flow maldistribution in the header, and ignore the stress change caused by the size.



*Figure 9. A schematic view of the header depth study.*

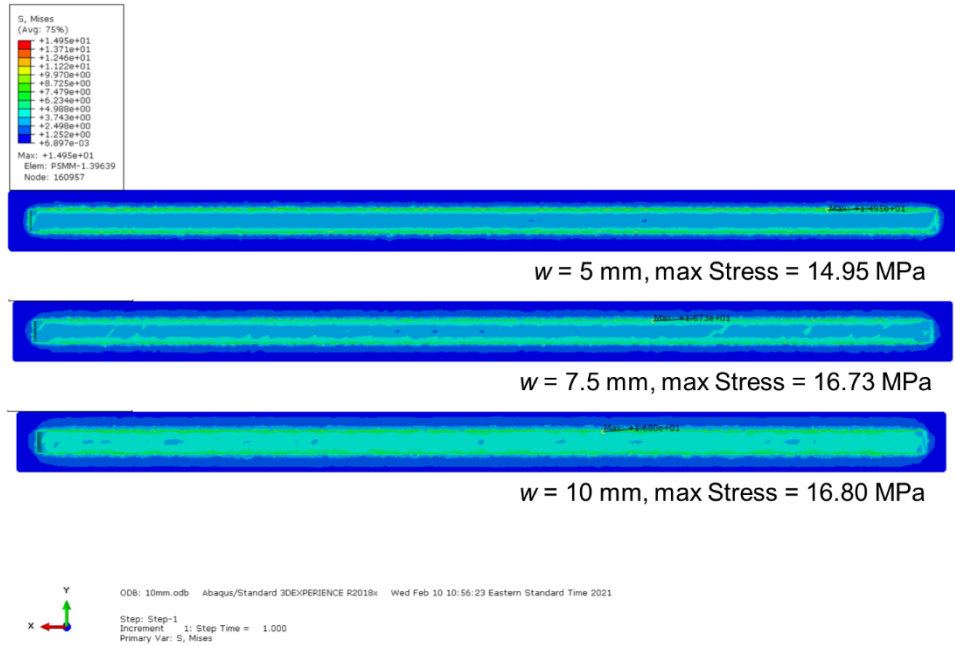
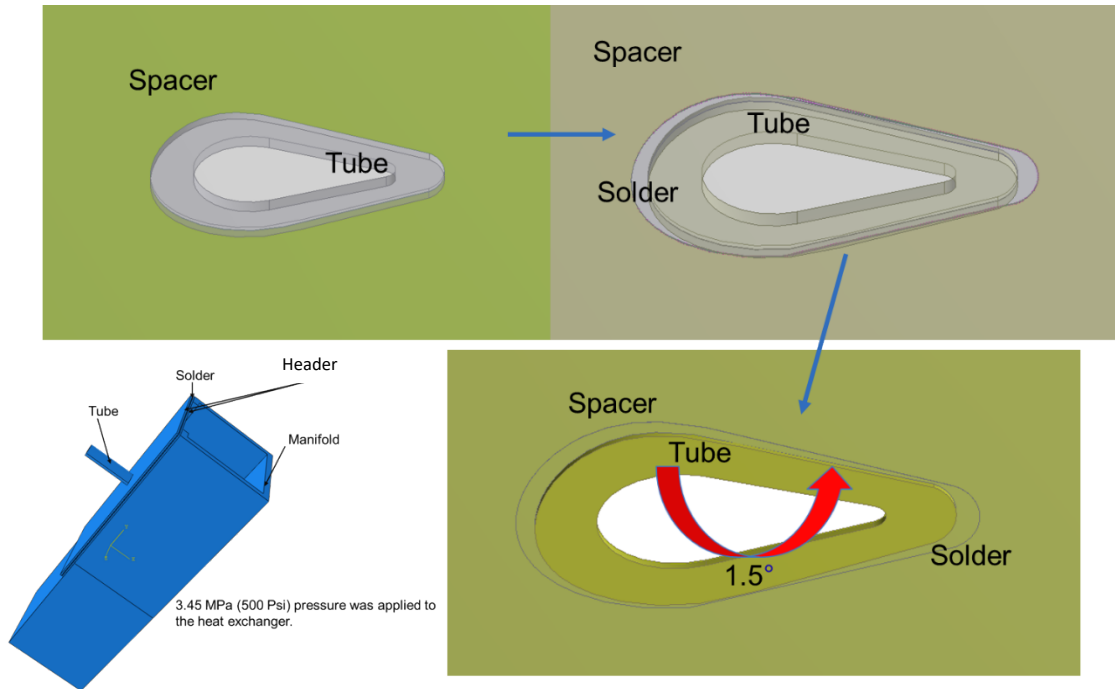


Figure 10. Stress distributions at the same cross-section of 3 headers with different size.

## 5. EFFECTS OF UNPERFECT FITTING OF THE SPACER AND TUBE

### *EFFECTS OF UNPERFECT FITTING OF THE SPACER AND TUBE*

Since in real fabrications, tubes will not perfectly fit the holes in the spacer, which may lead to a stress concentration. It is desired to investigate the effect of tubes fitting the holes. A case was designed as shown in Figure 11. In the case, the tube rotates 1.5 degrees from the original orientation and creates an uneven distribution of the solder. Then 3.45 MPa pressure was applied to the heat exchanger. The tube and spacer are made of copper while the solder is aluminum. Figures 12 and 13 show the stress distribution in the solder with original orientation and 1.5 degrees rotation respectively. The highest stresses from the two cases are 113 and 134 MPa, respectively. The results indicate that the rotation of the tube position in the solder will increase the stress in the solder.



*Figure 11. A case with 1.5 degrees rotation of the tube from the original orientation.*



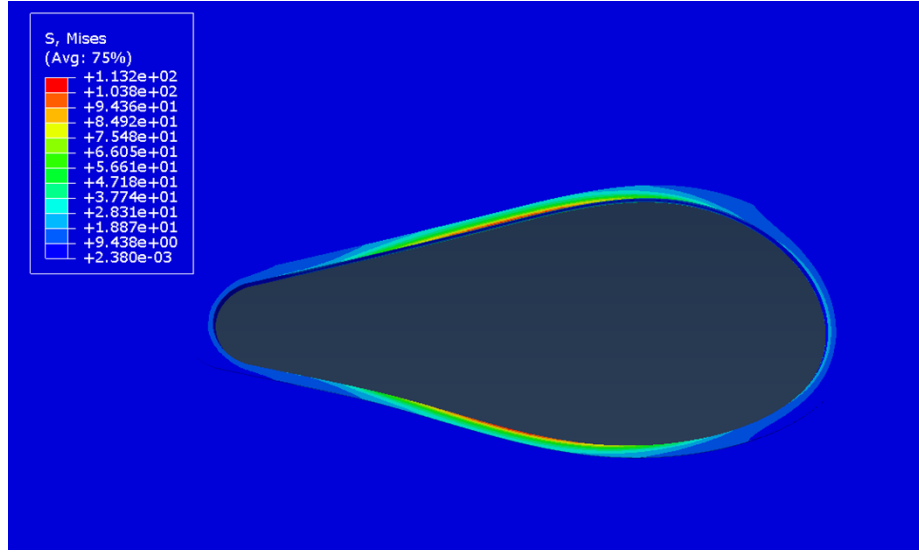


Figure 12. Stress distribution in the solder with original orientation.

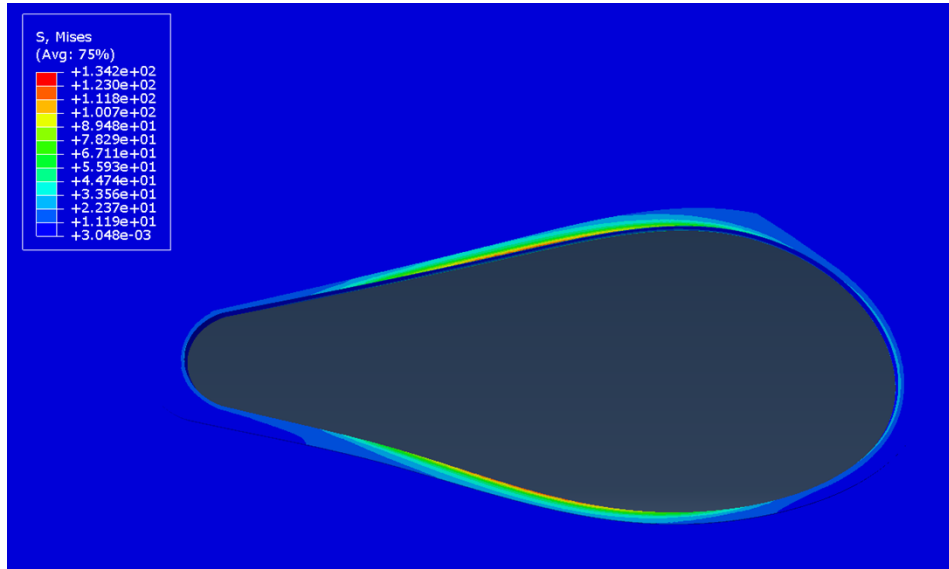


Figure 13. Stress distribution in the solder with 1.5 degrees rotation.

### **PLASTIC STRAIN ON THE SOLDER**

Since the stress is high on the solder between the spacer and tube in the heat exchanger (about 130 MPa), in which the strain of the solder may be beyond the elastic region. Therefore, it is necessary to conduct a study on the plastic strain on the solder. Same model was used as shown in Figure 11. In the heat exchanger, the solder is made of SAC 396 (Alloy: Sn95.5Ag3.9Cu0.6), while the other parts are made of copper. Then two real plastic stress-strain curves are employed to describe the relationship of plastic stress and strain for two solder alloys, SAC 396 and copper, with yield stress 35 MPa and 120 MPa, respectively as shown in Figure 14. Figures 15 and 16 depict the plastic stress and strain on the solder. If we use SAC 396 as the solder (yield stress = 35 MPa), the highest stress on the solder will be the yield stress, indicating

the energy has been transferred to the plastic deformation. The simulation result also shows that the highest plastic strain is about  $3 \times 10^{-3}$ .

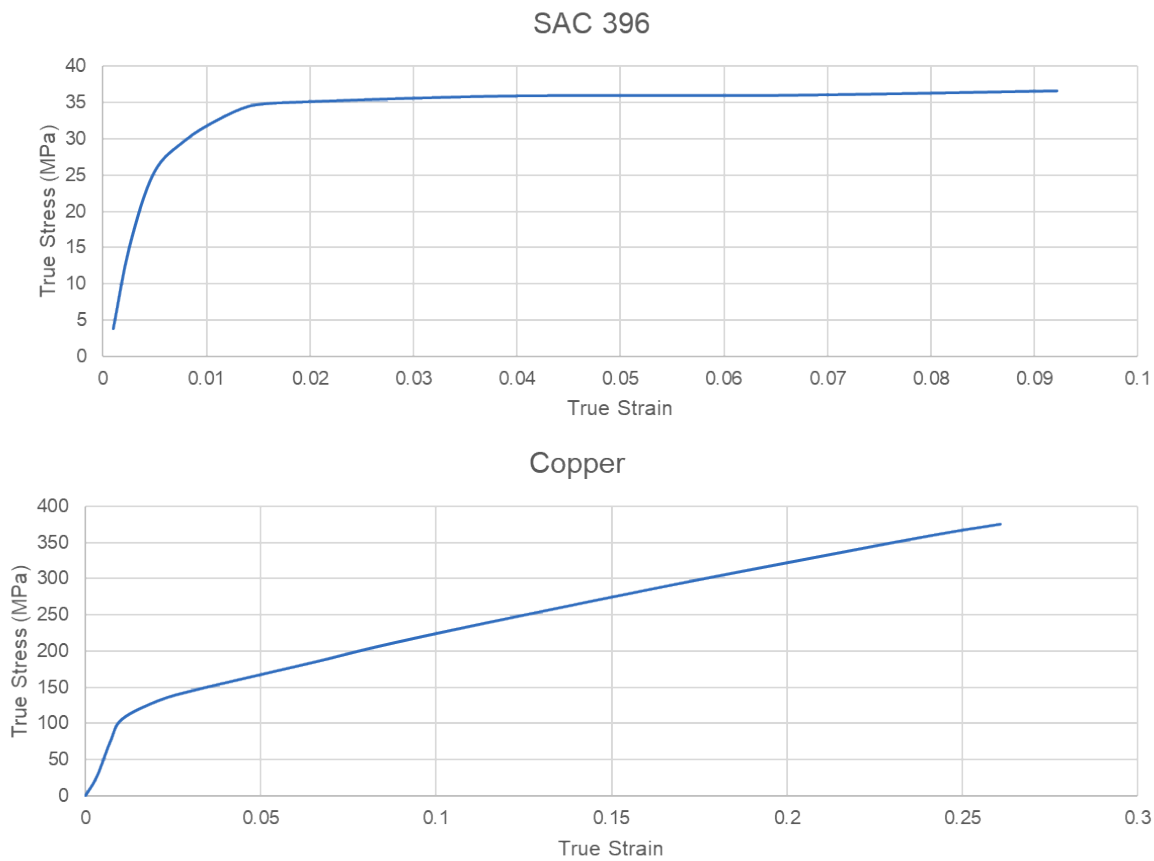


Figure 14. Plastic stress VS plastic strain for SAC 396 and copper.

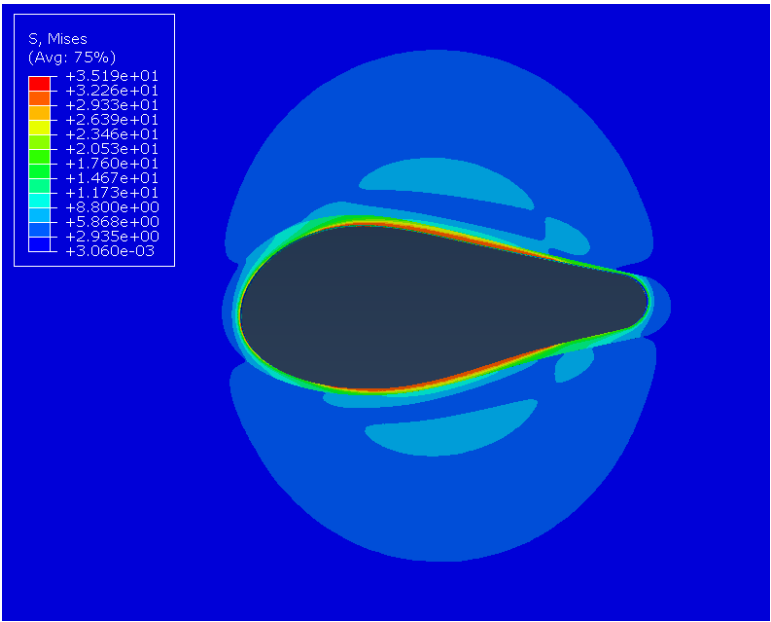
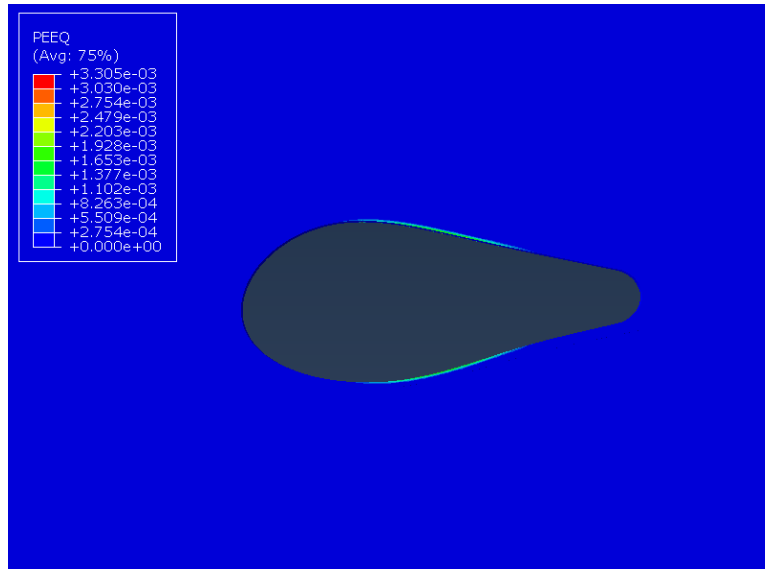


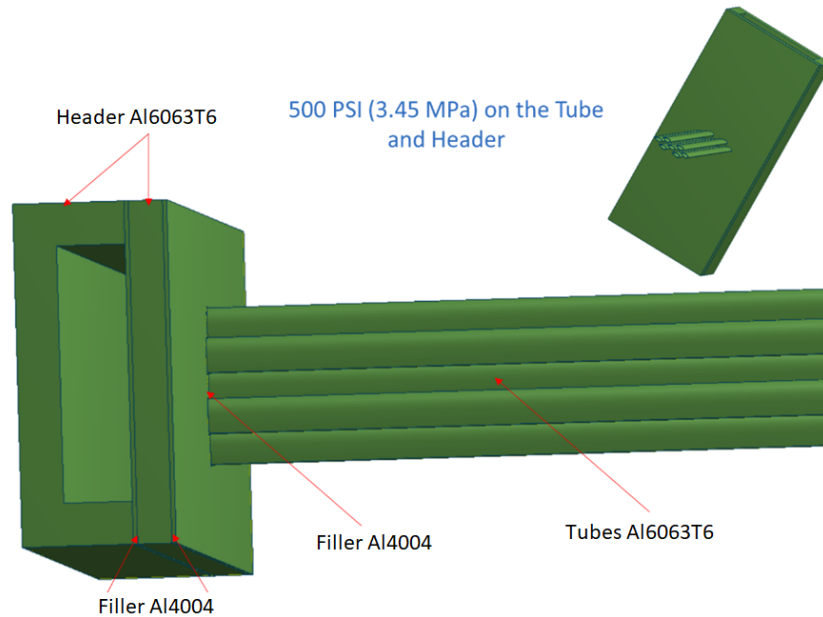
Figure 15. Plastic stress on the solder using SAC 396.



*Figure 16. Plastic strain on the solder using copper.*

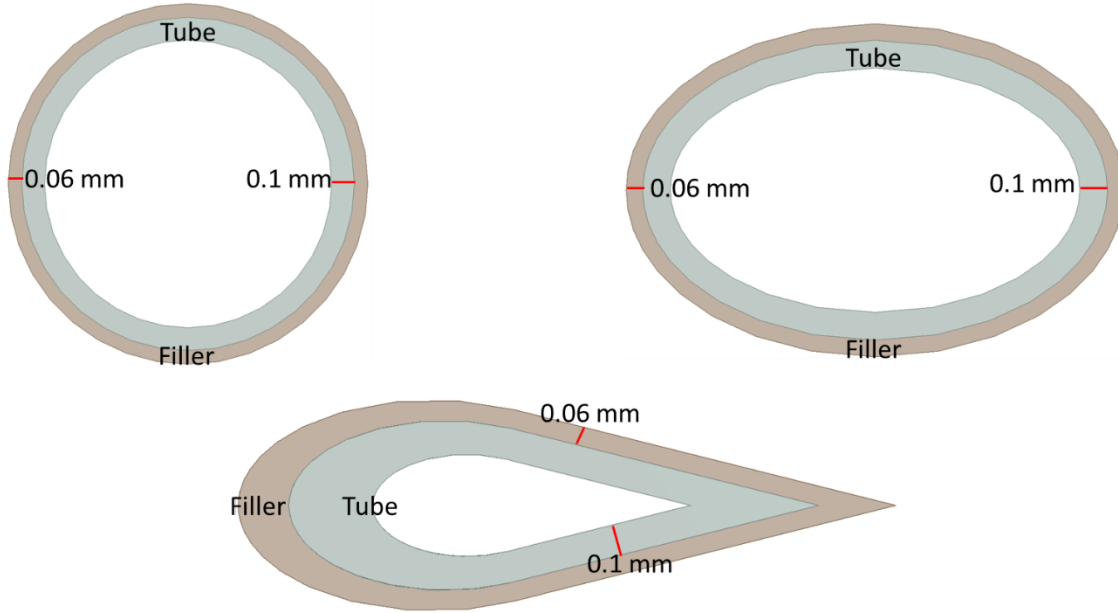
## 6. FATIGUE ANALYSIS OF ASSEMBLED HEAT EXCHANGERS.

Figure 17 shows a schematic view of the air-to-refrigerant heat exchanger studied in this section, which is comprised tubes and two headers at the two ends of each tube. Tubes connected to the header through a layer of filler as the joining material (e.g. solder). To save the computational resource, some simplifications have been applied. Due to the symmetric geometry of the heat exchanger, only a half of the heat exchanger is modeled. Moreover, only 7 tubes are included in the model instead of more than 100 tubes in the original heat exchanger since a preliminary test reveals that 7-tube model can capture the stress changes due to interactions between tube. As a result, the locations, and values of highest stress from 7-tube model is very close to the ones in the modeling including more than 100 tubes. Therefore, the 7-tube model can be used to represent the original heat exchanger to conduct the stress analysis. The materials of filler and tube/header are Al4004 and Al6063-T6, respectively. To mimic the inner pressure of an air-to-refrigerant heat exchanger, 3.45 MPa (500 PSI) pressure is applied to the inner surfaces of the tubes and header.



*Figure 17. Schematic view of the heat exchange model.*

In this section tube. The cross-sections of the tubes are shown in Figure 18. Since the tubes connect with the head using the filler, therefore, there exists a thin layer of filler between the tube and header, which are depicted as brown layers in Figure 18. Note the filler's outer perimeters of the three shapes are same about 5 mm, while the thicknesses of the filler and tube wall are 0.06 mm and 0.1 mm, respectively for all three shapes.



*Figure 18. Three shapes of the tubes and fillers.*

Figure 19 depicts the stress on the tubes for all three cases. Note only four of the seven tubes are shown in Figure 19. The highest stresses on round-shaped tubes, ellipse-shaped tubes, and airfoil-shaped tubes are 28.7 MPa, 189.1 MPa, and 84.1 MPa, respectively. The round tubes have the lowest stress because the stress concentration is hard to generate at the round-shaped cross section. The ellipse-shaped tubes, on the other hand, have the highest stress, which locate at the vertices of the ellipse cross-section. It is because stress concentrates at the vertices of the ellipse shape and generates high stress regions near them. The stresses on the airfoil-shaped tubes are lower stress than ellipse-shaped. It is not surprised that the highest stress occurs neat the tip of airfoil, since the sharp tip causes stress concentration. However, the tip shape merges upper and lower surfaces of the airfoil shaped tube, leading to the highest thickness part of the tube, which moderates the strength of stress concentration. As a result, the highest stress on the airfoil-shaped tubes is higher than the round-shaped ones but lower than the ellipse-shaped ones.

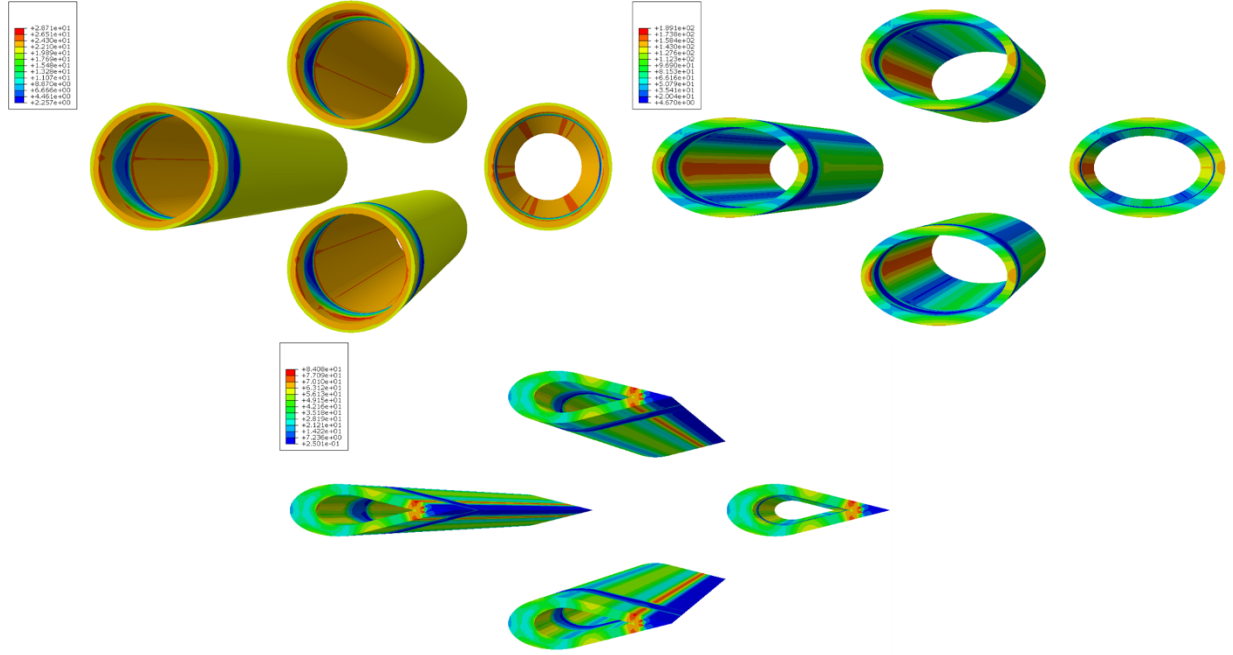


Figure 19. Stress distributions on the tubes with three shapes.

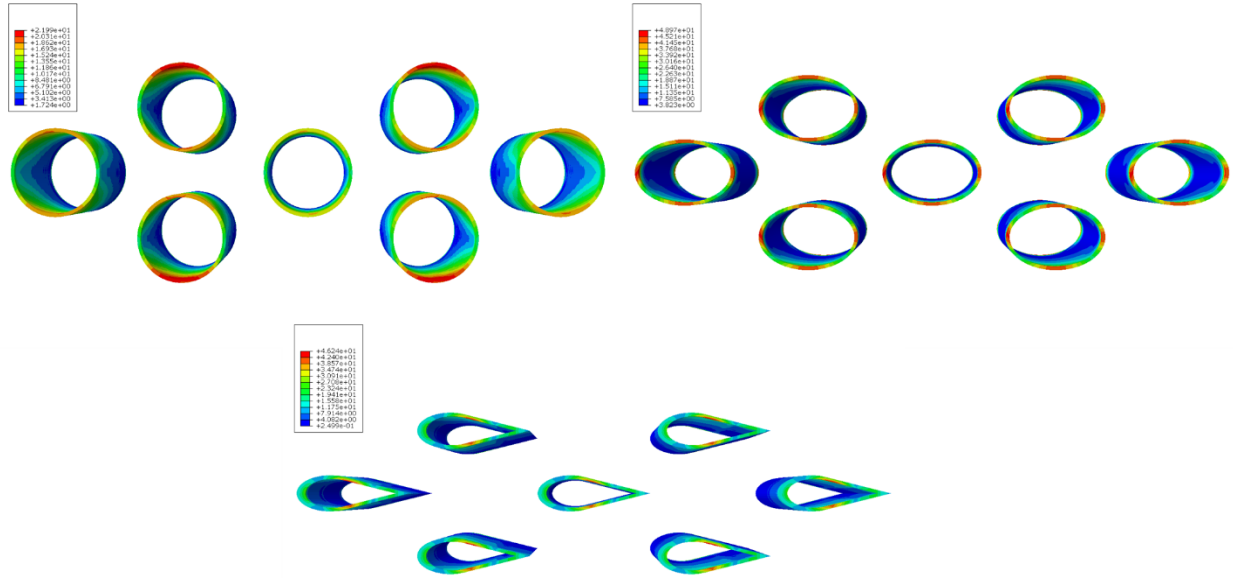


Figure 20. Stress distributions on the fillers with three shapes.

The filler is a thin layer of material (about 0.06 mm in present work) used to connect the tubes and headers. The stress distributions on the fillers for all three cases are shown in Figure 20. The highest stresses on the round-shaped fillers, ellipse-shaped fillers, and airfoil-shaped fillers are 22.1 MPa, 49.0 MPa, and 46.2 MPa, respectively. The round-shaped fillers have the lowest stresses which are much lower than the ellipse-shaped ones and airfoil-shaped ones. The locations of the highest stresses are different between fillers and tubes. The

highest stresses on the ellipse-shaped fillers happen not only near the vertices but also near co-vertices. On the other hand, the highest stresses on the airfoil-shaped fillers occur near the edges of upper and lower surfaces instead of the tip. The location differences of highest stress are because the pressure is applied to the tubes directly and then passed to the fillers. Therefore, the highest stresses occur the connection points between tubes and fillers.

Figure 21 shows the stress distributions on the headers for all three cases, in which the highest stress is less than 18 MPa. Note that the green background indicates that the most part of each header has about 7 MPa stress, which comes from the pressure applied to the header directly. Some low stress areas can be found between holes, which is due to the interactions between two applied stress creating low stress regions.

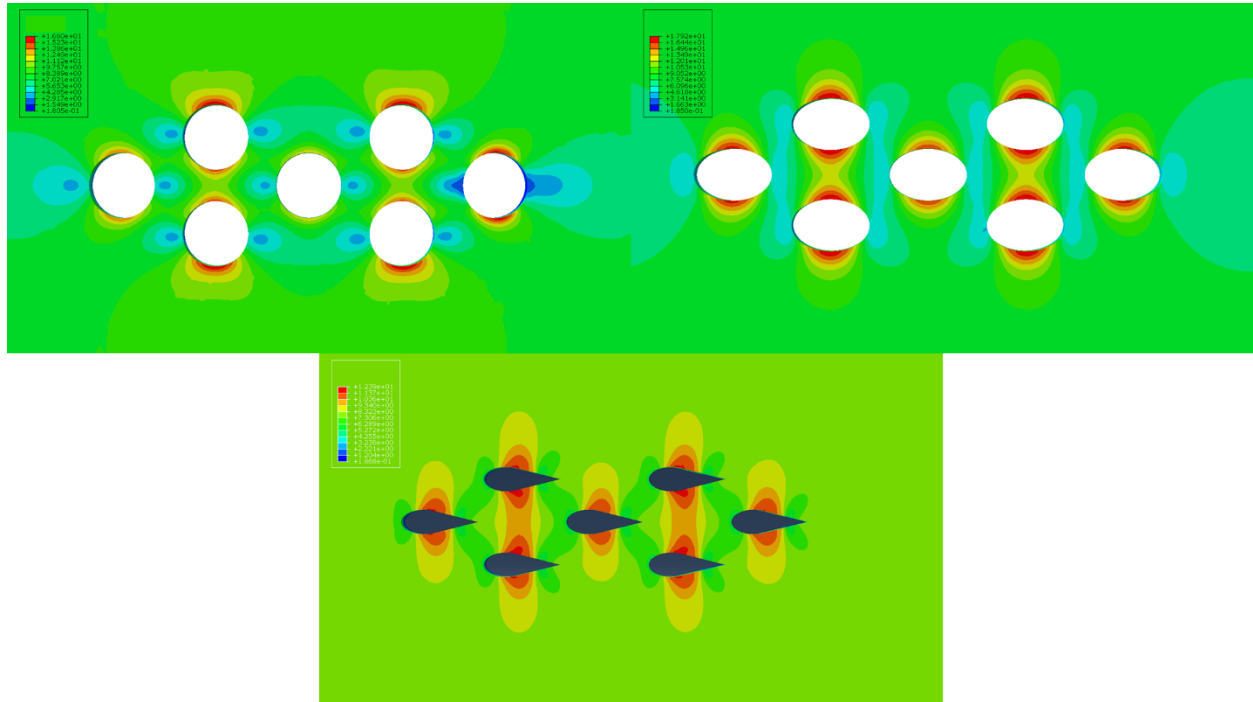


Figure 21. Stress distributions on the headers with three shapes.

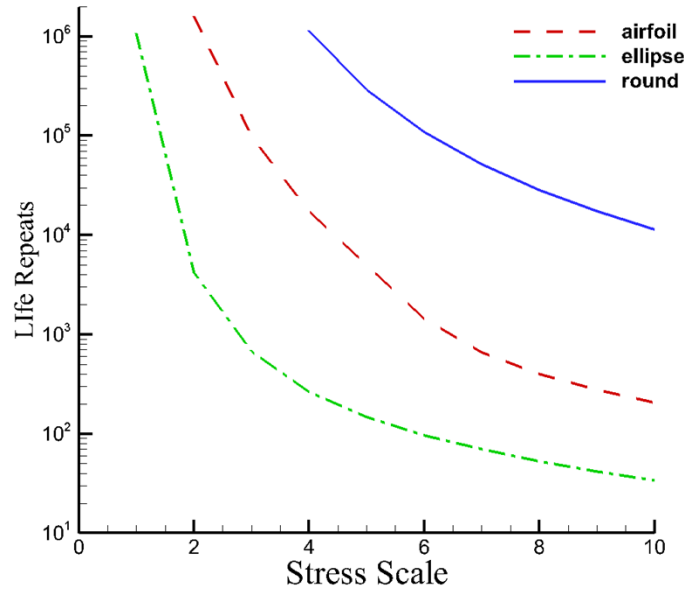


Figure 22. Fatigue analysis results showing life repeats vasus stress scale of the heat exchangers with three tube shapes.

After the stress analysis finished, the results were used to conduct fatigue analysis. In the fatigue analysis, a 1-0 stress curve is implemented, i.e. the stress switches repeatedly from 1 to 0 then back to 1, in which 1 and 0 indicate the stress on the heat exchanger from the stress analysis and no stress on the heat exchanger, respectively. Moreover, the stress on the heat exchanger is also scaled up to 10 times in the fatigue analysis. The output of the stress analysis is the life repeats of the heat exchanger, which indicates the repeats of the 1-0 cycles when the failure happens. Figure 22 shows the curve of life repeats vs stress scale times. Since the stress on the ellipse-shaped heat exchanger is the highest, it has a shortest life repeat, about 1 million repeats without stress scale and 34 repeats with 10 times stress scale. If it is assumed a typical, steady-state compressor cycle is about 40 minutes with the duty cycle, it can be calculated that it will take about 38 years for an ellipse-shaped heat exchanger failure happening due to the repeatedly 3.45 MPa pressure applied. The other two shapes' lifetimes are even longer.



## 7. SUMMARY

A framework of stress analysis and fatigue analysis of high-performance heat exchangers with non-round shaped tubes has been developed. The framework includes CAD model design by SOLIDWORKS, stress analysis model creation by ABAQUS, stress analysis model simulation by ABAQUS, and fatigue analysis by fe-safe. The stress analysis model has been validated by comparing to the experimental data. Then the framework is implemented to analyze the stress and fatigue for the parts of high-performance heat exchangers, including tube, header, and welding layer, as well as for the assembled heat exchanger. Some conclusions are summarized as following,

1. The fatigue analysis on the four different tube hole designs reveals that the tube lifetime can be improved by changing the tube hole from single ellipse to other shapes. The results also show that dual-round hole design leads to the longest lifetime of the tube.
2. The stress analysis on the three different cross-sections of the header indicates that the stress on the round-shaped header is the lowest among the three shapes under the same conditions. In addition, the study about the depth of the header shows that the depth does not have significant impact on the stress.
3. The framework was also used to reveal the effects of unperfect fitting of the spacer and tube. The results indicate about 20% increment of the stress on the welding layer when the tube rotates about 15°.
4. Finally, the framework was implemented to conduct fatigue analysis on the assembled heat exchangers with different tube shapes, including round, ellipse, and airfoil shapes. The fatigue analysis indicates that although the heat exchanger with the ellipse-shaped tubes has the worst life repeats among the three heat exchangers, it still can work more than 38 years without failure under repeatedly 3.45 MPa pressure applied

## REFERENCES

- Bacellar, Daniel, Vikrant Aute, Zhiwei Huang, and Reinhard Radermacher. 2016. “Novel Airside Heat Transfer Surface Designs Using an Integrated Multi-Scale Analysis with Topology and Shape Optimization.” in *International Refrigeration and Air Conditioning Conference*.
- Bacellar, Daniel, Vikrant Aute, Zhiwei Huang, and Reinhard Radermacher. 2017. “Design Optimization and Validation of High-Performance Heat Exchangers Using Approximation Assisted Optimization and Additive Manufacturing.” *Science and Technology for the Built Environment* 23(6):896–911.
- Bäumel, Anton, T. Seeger, and Chr Boller. 1990. *Materials Data for Cyclic Loading: Supplement 1*. Elsevier.
- Huang, Zhi Wei, Zhen Ning Li, Yunho Hwang, and Reinhard Radermacher. 2016. “Application of Entransy Dissipation Based Thermal Resistance to Design Optimization of a Novel Finless Evaporator.” *Science China Technological Sciences* 59(10):1486–93.